Impact of Spikelets on Hippocampal CA1 Pyramidal Cell Activity During Spatial Exploration

Jérôme Epsztein, *et al.*

Science **327**, 474 (2010);
DOI: 10.1126/science.1182773

rently in use (*21*–*26*), confirming clinical practice as a major driver of pathogen evolution and lending heightened importance to understanding the relevance of other homoplasies. Such insights inform future surveillance strategies for the detection of emerging clones and management of epidemic spread. We fully anticipate that, as the technology and analytical methods improve, the approach described here will underpin the next wave of molecular data for epidemiological and microevolutionary studies in bacteria.

References and Notes

1. M. C. Maiden *et al.*, *Proc. Natl. Acad. Sci. U.S.A.* **95**, 3140 (1998).
2. M. C. Enright *et al.*, *Proc. Natl. Acad. Sci. U.S.A.* **99**, 7687 (2002).
3. B. L. Xu *et al.*, *J. Hosp. Infect.* **71**, 245 (2009).
4. E. J. Feil *et al.*, *J. Clin. Microbiol.* **46**, 1520 (2008).
5. E. Alp *et al.*, *J. Infect.* **58**, 433 (2009).
6. K. S. Ko *et al.*, *J. Clin. Microbiol.* **43**, 421 (2005).
7. D. C. Oliveira, A. Tomasz, H. de Lencastre, *Microb. Drug Resist.* **7**, 349 (2001).
8. A. M. Vivoni *et al.*, *J. Clin. Microbiol.* **44**, 1686 (2006).
9. M. D. Bartels *et al.*, *Eur. J. Clin. Microbiol. Infect. Dis.* **27**, 757 (2008).
10. A. Szczepanik, M. Kozioł-Montewka, Z. Al-Doori, D. Morrison, D. Kaczor, *Eur. J. Clin. Microbiol. Infect. Dis.* **26**, 29 (2007).
11. O. Melter *et al.*, *J. Clin. Microbiol.* **41**, 4998 (2003).
12. Materials and methods are available as supporting material on *Science* Online.
13. J. A. Lindsay, M. T. G. Holden, *Trends Microbiol.* **12**, 378 (2004).
14. J. D. Edgeworth *et al.*, *Clin. Infect. Dis.* **44**, 493 (2007).
15. H. de Lencastre, A. Tomasz, in *Evolutionary Biology of Bacterial and Fungal Pathogens*, F. Baquero, C. Nombela, G. H. Cassell, J. A. Gutierrez, Eds. (American Society for Microbiology, Washington, DC, 2008), pp. 333–346.
16. H. Ochman, S. Elwyn, N. A. Moran, *Proc. Natl. Acad. Sci. U.S.A.* **96**, 12638 (1999).
17. N. A. Moran, H. J. McLaughlin, R. Sorek, *Science* **323**, 379 (2009).
18. D. Falush *et al.*, *Proc. Natl. Acad. Sci. U.S.A.* **98**, 15056 (2001).
19. E. P. Rocha *et al.*, *J. Theor. Biol.* **239**, 226 (2006).
20. U. Nübel *et al.*, *Proc. Natl. Acad. Sci. U.S.A.* **105**, 14130 (2008).
21. S. Besier, A. Ludwig, V. Brade, T. A. Wichelhaus, *Mol. Microbiol.* **47**, 463 (2003).
22. G. E. Dale *et al.*, *J. Mol. Biol.* **266**, 23 (1997).
23. J. G. Hurdle, A. J. O'Neill, I. Chopra, *J. Antimicrob. Chemother.* **53**, 102 (2004).
24. M. Tanaka, T. Wang, Y. Onodera, Y. Uchida, K. Sato, *J. Infect. Chemother.* **6**, 131 (2000).
25. A. A. Vickers, N. J. Potter, C. W. Fishwick, I. Chopra, A. J. O'Neill, *J. Antimicrob. Chemother.* **63**, 1112 (2009).
26. T. A. Wichelhaus *et al.*, *Antimicrob. Agents Chemother.* **46**, 3381 (2002).
27. D. Harmsen *et al.*, *J. Clin. Microbiol.* **41**, 5442 (2003).

28. The Sanger Institute is core funded by the Wellcome Trust. We thank C. Milheiriço and J. D. Cockfield for preparation of genomic DNA and G. Dougan and the Sanger Institute Sequencing and Informatics groups for general support. S.G. and A.T. were supported by grants SFRH/BPD/25403/2005 and SFRH/BD/44220/2008, respectively, from Fundação para a Ciência e Tecnologia, Portugal. E.K.N., N.C., N.D., and S.J.P. were funded by the Wellcome Trust. Funding for the sequencing of the TW20 genome was provided by Guy's and St. Thomas' Charity. J.D.E. receives funding from the Department of Health via the National Institute for Health Research's comprehensive Biomedical Research Centre award to Guy's and St. Thomas' National Health Service Foundation Trust in partnership with King's College London. The Illumina Genome Analyzer reads are deposited in the Short Read Archive (National Center for Biotechnology Information) under the accession no. ERA000102. The annotated chromosome of TW20 has been submitted to European Molecular Biology Laboratory with the accession number FN433596.

Supporting Online Material

www.sciencemag.org/cgi/content/full/327/5964/469/DC1
Materials and Methods
Figs. S1 to S4
Tables S1 to S4

24 September 2009; accepted 25 November 2009
10.1126/science.1182395

Impact of Spikelets on Hippocampal CA1 Pyramidal Cell Activity During Spatial Exploration

Jérôme Epsztein,*† Albert K. Lee,*‡ Edith Chorev, Michael Brecht

In vivo intracellular recordings of hippocampal neurons reveal the occurrence of fast events of small amplitude called spikelets or fast prepotentials. Because intracellular recordings have been restricted to anesthetized or head-fixed animals, it is not known how spikelet activity contributes to hippocampal spatial representations. We addressed this question in CA1 pyramidal cells by using in vivo whole-cell recording in freely moving rats. We observed a high incidence of spikelets that occurred either in isolation or in bursts and could drive spiking as fast prepotentials of action potentials. Spikelets strongly contributed to spiking activity, driving ~30% of all action potentials. CA1 pyramidal cell firing and spikelet activity were comodulated as a function of the animal's location in the environment. We conclude that spikelets have a major impact on hippocampal activity during spatial exploration.

Spikelets are voltage fluctuations of small amplitude with a spike-like waveform. They were initially described in in vivo intracellular recordings from the hippocampus and inferior olive of anesthetized animals (*1*, *2*). Further in vitro experimental work using paired recordings has shown that spikelets can result from direct action potential transmission via electrical coupling between principal cells (*3*, *4*) and interneurons (*5*–*12*). In the hippocampus, it has been suggested that such coupling can occur between the axons of principal neurons (*13*, *14*). However, it has also been suggested that spikelets could reflect the occurrence of ectopic axonal spikes (*15*–*17*) or dendritic spikes (*1*), and the exact origin of spikelet activity remains to be clarified. Because spikelets are difficult to detect with extracellular techniques classically used to record neuronal activity in freely moving animals, nothing is known about how these events contribute to hippocampal spatial representations (*18*, *19*). To address this question, we used head-anchored whole-cell recording in freely moving rats (*20*–*23*) and analyzed spikelet activity during spatial exploration (*22*).

Recordings were performed in current clamp mode while the animal freely explored an O-shaped maze. We first characterized the properties of hippocampal spikelets (Fig. 1). In an identified CA1 pyramidal cell (Fig. 1A), we observed fast all-or-none events of small amplitude (Fig. 1B, upper trace) that occurred at high frequency (mean = 4.96 Hz) while the rat ran around the maze (Fig. 1B, lower trace). In 10 neurons, these events had electrophysiological characteristics (Fig. 1C) matching those of previously described spikelets such as a fast rise time (mean ± SEM = 0.56 ± 0.08 ms), a biphasic decay ($\tau1$ = 0.87 ± 0.11 ms; $\tau2$ = 17.3 ± 5.2 ms), a small amplitude (mean = 7.03 ± 1.00 mV), and all-or-none behavior. Spikelets had much faster kinetics and higher amplitude ($P < 0.01$) than did excitatory postsynaptic events recorded in the same cells (Fig. 1, D and E, and fig. S1). On the other hand, they were much slower and smaller ($P < 0.001$) than action potentials (APs) (Fig. 1F and fig. S1).

Spikelets were found in a majority of recorded CA1 pyramidal cells (10 out of 16 cells) and occurred with a mean frequency of 4.8 ± 1.6 Hz. Spikelets could be observed either isolated or in the form of short bursts (mean burst duration = 19 ± 1 ms; Fig. 2, A and B). Bursts consisted of three to six spikelets (mean = 3.2 ± 0.4) at high frequency (mean = 138 ± 9 Hz, Fig. 2C) often embedded with APs (in five cells with spikelet bursts).

How are spikelets related to the neuron's suprathreshold activity? To address this, we first

Bernstein Center for Computational Neuroscience, Humboldt University, 10115 Berlin, Germany.

*These authors contributed equally to this work.
†Present address: Institut de Neurobiologie de la Méditerranée, Institut National de la Santé et de la Recherche Médicale U901, Parc scientifique et technologique de Luminy, Boîte Postale 13, 13273 Marseille Cedex 9, France. To whom correspondence should be addressed. E-mail: epsztein@inmed.univ-mrs.fr
‡Present address: Howard Hughes Medical Institute, Janelia Farm Research Campus, Ashburn, VA 20147, USA.

analyzed whether spikelets contribute to AP activity. Spikelets could be recorded as fast prepotentials of APs as previously described (*1*, *2*, *24*) (Fig. 3A). Close examination (Fig. 3B) revealed two populations of APs in our data set: some starting abruptly from a slowly rising baseline membrane potential (we refer to them as full-blown APs, fb-APs) and some starting with a faster initial rising phase (we refer to this second class of APs as shoulder APs, sh-APs). When the first derivative (*dV/dt*) of the AP was computed (Fig. 3C), a characteristic initial rising phase (shoulder potential) was seen before the threshold for sh-APs, whereas no such shoulder was observed for fb-APs or APs evoked by current step injection. The distinction between fb-APs and sh-APs became much clearer when the rate of rise of the membrane potential in the 1 ms immediately preceding the AP threshold (50 V/s) was computed (fig. S2).

A number of observations suggest that sh-APs are actually APs initiated by spikelets: Spikelets and shoulder potentials had (i) similar rates of rise (12.5 ± 2.4 versus 13.1 ± 2.6 V/s; $P = 0.78$), (ii) similar peak *dV/dt* (15.1 ± 3.6 versus 19.1 ± 7.5 V/s; $P = 0.90$), and (iii) sh-APs were never seen in cells that had no spikelet activity (n = 6 out of 6) (fig. S3). That spikelets are sufficient to trigger spikes is strongly supported by the temporal correlation of all spikelet (including shoulder potentials) and AP activity. As shown in the spikelet-AP crosscorrelogram (Fig. 3, D and E), APs were tightly time-locked to spikelets, suggesting that it is the occurrence of the spikelet rather than other inputs that ultimately drives those APs. In addition to the sharp millisecond time scale locking of spikelets and AP activity, we also observed a broader temporal correlation on the 10-ms time scale. As stated above, spikelets often occurred in the form of high frequency bursts with interspikelet intervals in that range (range from 6.1 to 9 ms, $n = 5$). The modulation of the spikelet-AP crosscorrelogram with similar intervals is in line with the idea that a large proportion of APs are driven by spikelets. To further test that sh-APs are driven by spikelets, we also performed current injection experiments in four neurons with spikelets in anesthetized animals and computed the spikelet-to-AP transfer ratio (the ratio of shoulder potentials to all spikelets, including both isolated spikelets and the ones in the form of shoulder potentials). We observed a significant increase in the spikelet-to-AP transfer ratio during depolarization by current injection in two of these neurons (we could not assess the effect of current injection in a statistically meaningful way in the two remaining cells) (fig. S4).

We then quantified the occurrence of sh-APs in CA1 pyramidal cells. Sh-APs could be ob-

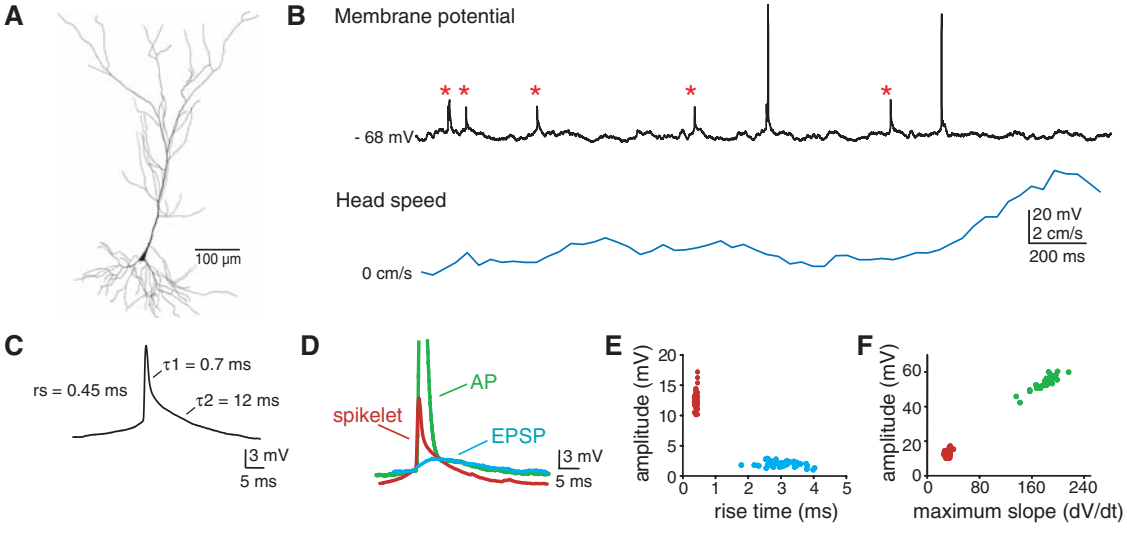

Fig. 1. Spikelets from an identified hippocampal CA1 pyramidal cell in a freely moving rat. (**A**) Reconstruction of the morphology of the recorded CA1 pyramidal neuron filled with biocytin during recording. (**B**) (Top) Membrane potential trace recorded during spatial exploration. Fast events of small amplitude (red stars) are present in addition to action potentials (APs). (Bottom) Corresponding speed of the animal's head. (**C**) Averaged spikelet (n = 35). Mean spikelet has a fast rise time (rs) and a decay time best fitted by the sum of two exponentials. (**D**) Superimposition of averaged APs (green), spikelets (red), and excitatory postsynaptic potentials (EPSPs, blue). (**E**) Scatterplot of EPSP (blue) and spikelet (red) amplitude versus rise time. Spikelets represent an independent population of events with faster rise times and larger amplitudes than EPSPs. (**F**) Scatterplot of AP (green) and spikelet (red) amplitude versus maximum rising slope (*dV/dt*). Spikelets represent an independent population of events with slower rising slopes and smaller amplitudes than APs.

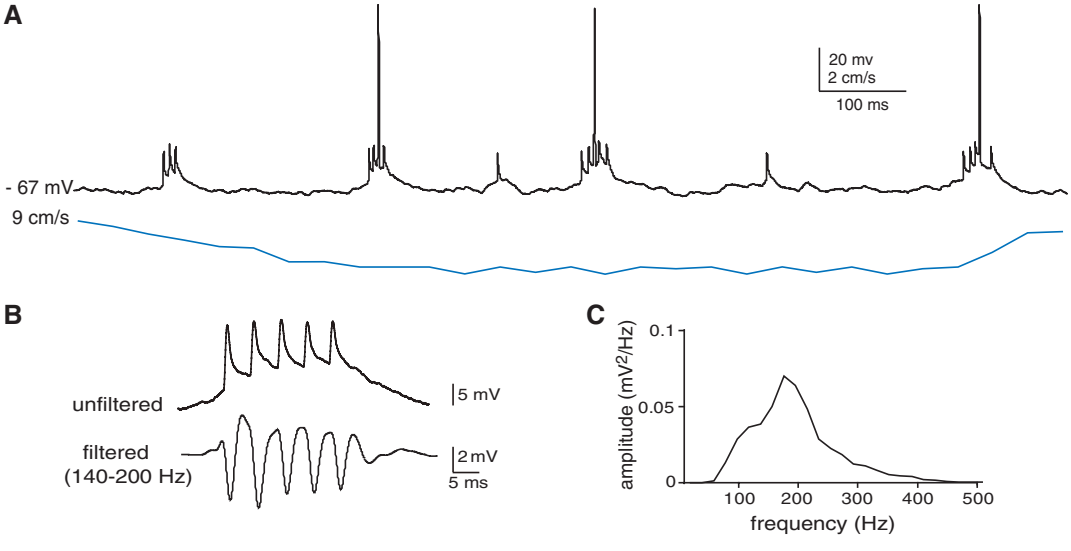

Fig. 2. Temporal pattern of spikelets. (**A**) (Top) Membrane potential trace of a CA1 pyramidal cell during spatial exploration. Spikelets often occur as high frequency bursts. (Bottom) Corresponding speed of the animal's head. (**B**) Example of a spikelet burst recorded in this cell. (Top) Unfiltered. (Bottom) Filtered in the ripple frequency band. (**C**) Mean power spectrum of spikelet bursts recorded in this cell (n = 49 bursts, mean interspikelet interval = 6.1 ± 1.5 ms).

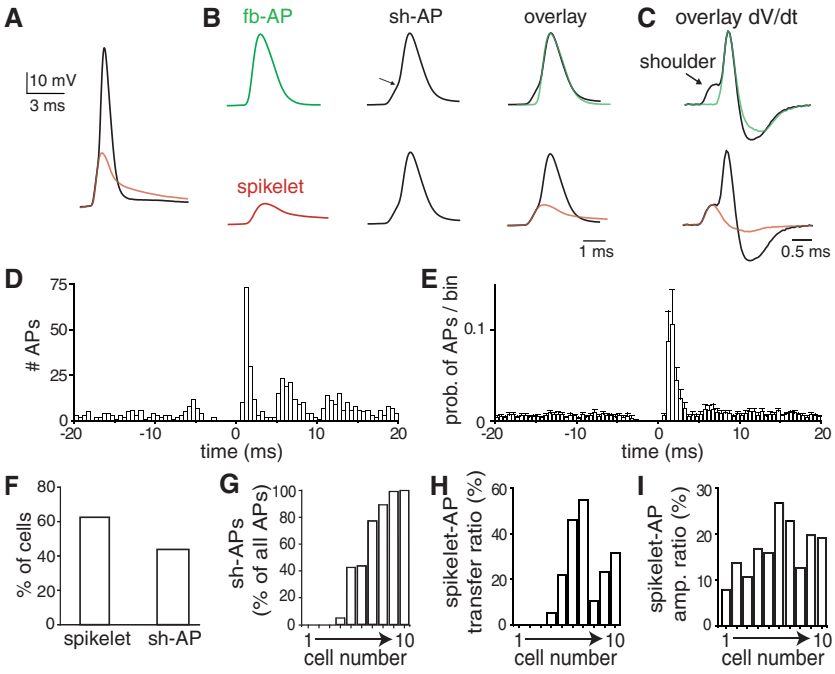

Fig. 3. Spikelets drive spiking in CA1 pyramidal cells in freely moving rats. (**A**) Overlay of mean AP (black) and spikelet (red) waveforms. (**B**) (Top) Mean waveforms of fb-APs (green) as evoked by current injection and sh-APs (black, shoulder break marked by an arrow), overlaid on the right. (Bottom) Mean waveforms of spikelets (red) and sh-APs (black), overlaid on the right. (**C**) (Top) Overlay of first derivative (*dV/dt*) of mean fb-AP as evoked by current injection (green) and sh-AP (black). (Bottom) Overlay of first derivative (*dV/dt*) of mean sh-AP (black) and spikelet (red). The shoulder potential corresponds to the spikelet waveform. (**D**) Spikelet-AP crosscorrelogram for the cell shown in Fig. 2. The start time of all spikelets (including the ones in the form of shoulder potentials) is cross-correlated with the peak time of all APs (fb-APs and sh-APs). (**E**) Same as in (D) for all cells with spikelets ($n = 10$). Error bars indicate SEM. (**F**) Fraction of cells with spikelets and sh-APs. (**G**) Fraction of sh-APs out of all APs (fb-APs and sh-APs) for each cell with spikelets. (**H**) Fraction of spikelets that drive spiking (in the form of shoulder potentials) out of all spikelets (isolated spikelets and shoulder potentials) for each cell with spikelets. (**I**) Spikelet amplitude expressed as a percentage of AP amplitude for each cell with spikelets.

served in a large proportion of recordings (7 out of 16 cells, Fig. 3F) and in these cells represented a large fraction of spiking activity (mean = 65 ± 13% of all APs; Fig. 3G). Across all cells (including those without spikelets), we found that spikelets triggered 28 ± 10% of the spiking activity of CA1 pyramidal cells in the awake behaving animal. As shown in Fig. 3G, the proportion of sh-APs varied greatly between cells with spikelets. We computed the spikelet-to-AP transfer ratio, which represents the efficiency with which spikelets drive APs, for individual cells (Fig. 3H) and observed that it could be predicted in part from the amplitude of the respective spikelets (Fig. 3I). Although in several cells close to 100% of APs were sh-APs, we never observed a cell where all spikelets resulted in sh-APs.

Lastly we analyzed the behavioral correlates of spikelets. Extracellular recordings have revealed a strong spatial modulation of hippocampal CA1 pyramidal cell firing (*18*, *19*). In our data set, there were seven cells in which the animal completed multiple laps around the maze and which we analyzed for such place cell activity (*23*, *25*). Of these, three (~40%) were place cells, showing spatial modulation of their firing rate. Figure 4 shows an example of such a cell where spikelet and sh-AP activity were detected. The cell showed an increase in AP firing rate during two successive passes through the same location (i.e., its place field). The frequency of both fb-APs and spikelets was specifically increased in this location (Fig. 4, A and B, and fig. S5A). The sh-AP rate was also specifically increased in the same location, indicating that spikelet activity contributed to spiking activity

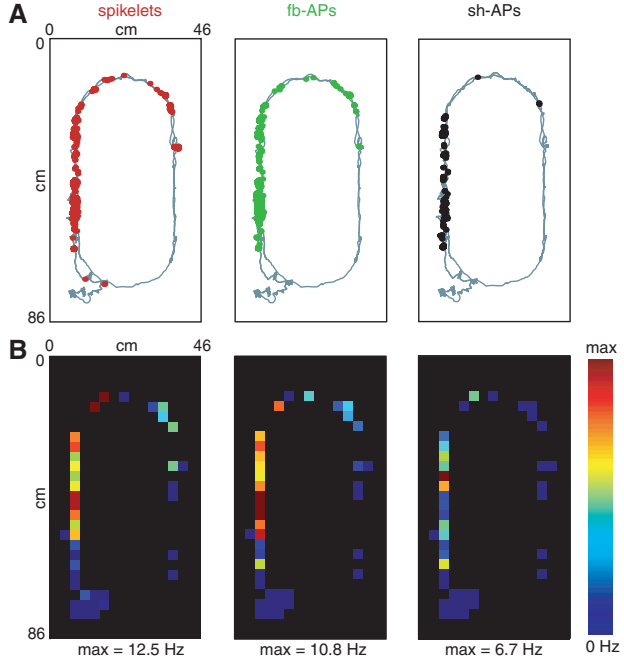

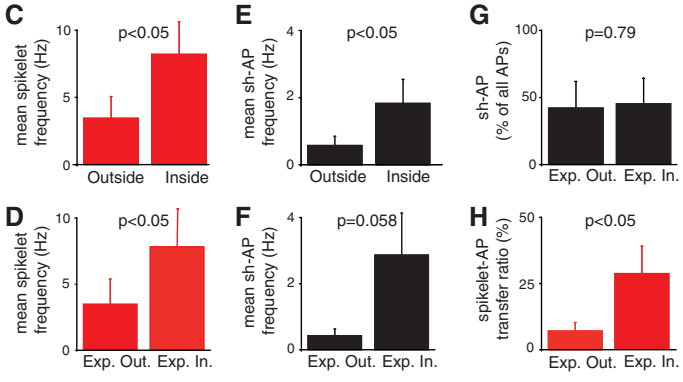

Fig. 4. Spatial correlates of spikelets and APs in CA1 pyramidal cells of freely moving rats. (**A**) Firing locations of isolated (nonshoulder) spikelets (left, red dots), fb-APs (middle, green dots), and sh-APs (right, black dots) while a rat was running in an O-shaped maze (inner wall not depicted; gray, trajectory of the animal during the recording). (**B**) Color-coded rate maps for the events in (**A**) (3-cm by 3-cm bins, maximum firing rate indicated below). (**C**) Bar graph of the mean spikelet frequency when the rat is outside versus inside the place field. Error bars indicate SEM. (**D**) Bar graph of the mean spikelet frequency when the rat is exploring (exp.) outside (out.) versus inside (in.) the place field. (**E**) Bar graph of the mean sh-AP frequency when the rat is outside versus inside the place field. (**F**) Bar graph of the mean sh-AP frequency when the rat is exploring (exp.) outside (out.) versus inside (in.) the place field. (**G**) Bar graph of the mean proportion of sh-APs (out of all APs) when the rat is exploring (exp.) outside (out.) versus inside (in.) the place field. (**H**) Bar graph of the mean spikelet-AP transfer ratio when the rat is exploring (exp.) outside (out.) versus inside (in.) the place field.

recorded inside the place field (Fig. 4, A and B). In two out of the three recorded place cells, AP and spikelet activity were spatially comodulated, whereas the remaining cell showed no spikelet activity.

We also analyzed spiking and spikelet spatial modulation in four additional cells where the rat's spatial exploration was sufficient (i.e., a single lap around the maze) for spatial modulation analysis but which we could not unambiguously classify as place cells [because of the absence of data across multiple laps (*25*)]. The AP firing rate was spatially modulated in all four of these cells, and the spikelet rate in two. Remarkably, three of these cells showed significant spatial comodulation of spike and spikelet rate ($P < 0.05$, figs. S5B and S6). Overall, out of six spatially modulated cells with spikelets (two of which were classified as place cells), five showed significant ($P < 0.05$) comodulation. We conclude that, like spiking activity, spikelet activity can be spatially modulated in CA1 pyramidal cells and that both types of cellular activity are spatially aligned.

We then analyzed spikelet activity in the non–place-modulated cells. In these cells, the overall spiking activity was very low, as previously described (*26*). Interestingly, only one out of four non–place-modulated cells showed spikelet activity, and in this cell spikelet frequency was low (0.12 Hz). Furthermore, this cell showed no spatial modulation of spikelet activity.

Further analysis was done to investigate the specific functional contribution of spikelets to in-field spiking during spatial exploration. The animal's behavior was classified into periods of exploratory versus resting (but awake) behavior and separately into periods inside versus outside the AP firing rate field (*25*) for the six spatially modulated cells with spikelets. The mean spikelet firing rate was higher inside compared with outside the field (Fig. 4C), consistent with the spatial comodulation of AP and spikelet firing rates. This difference was preserved when considering only periods of exploratory behavior (7.82 Hz inside versus 3.50 Hz outside, $P < 0.05$; Fig. 4D). The in-field spikelet rate was not different between exploration and rest ($P = 0.53$), as was also the case for the out-of-field rate ($P = 0.98$) (Fig. 4D and fig. S7A). Thus, the spikelet rate depends on the animal's location with respect to the AP field regardless of behavioral state. What about the sh-APs, which represent the direct effect of spikelets on spiking? The mean sh-AP rate was higher inside versus outside the AP field (Fig. 4E), and this relation held during both exploration (2.86 Hz versus 0.43 Hz, $P = 0.058$; Fig. 4F) and rest (fig. S7B). However, the proportion of all APs that was driven by spikelets was not different inside versus outside the field during exploration (0.45 versus 0.42, $P = 0.79$, Fig. 4G) or rest (fig. S7C). In contrast, the spikelet-AP transfer ratio was higher inside versus outside the field during exploration (0.29 versus 0.07, $P < 0.05$, Fig. 4H) and similarly so, but by a lesser amount, during rest (fig. S7D). Thus, spikelets have their maximum impact on spiking within the place field during exploratory behavior. On the basis of the findings from our current injection experiments, we suggest that the increased efficacy of spikelets results from membrane potential depolarization inside the place field (*23*, *27*).

Spikelets have been observed in intracellular recordings of a variety of neuronal types both in vivo and in vitro. In the hippocampus, in vitro slice recordings as well as computational simulations suggest an important synchronizing role for spikelets during spontaneous high-frequency oscillations (*28*) and acute pharmacologically induced epileptiform activity (*29*–*33*). Here, intracellular recordings in freely behaving animals allowed us to assess the role of spikelet activity during spatial exploration. In hippocampal CA1 pyramidal cells with spatially modulated spiking, the frequency of spikelets was elevated within the place field; however, in those cells lacking clear spatial modulation of spiking, spikelet as well as spike frequency were both low. Together with the observation that spikelets can powerfully influence the spiking behavior of CA1 pyramidal cells, these results provide new insights into why hippocampal place cells fire where they fire.

References and Notes

1. E. R. Kandel, W. A. Spencer, *J. Neurophysiol.* **24**, 272 (1961).
2. R. Llinas, R. Baker, C. Sotelo, *J. Neurophysiol.* **37**, 560 (1974).
3. B. A. MacVicar, F. E. Dudek, *Science* **213**, 782 (1981).
4. A. Mercer, A. P. Bannister, A. M. Thomson, *Brain Cell Biol.* **35**, 13 (2006).
5. M. Galarreta, S. Hestrin, *Nature* **402**, 72 (1999).
6. J. R. Gibson, M. Beierlein, B. W. Connors, *Nature* **402**, 75 (1999).
7. P. Mann-Metzer, Y. Yarom, *J. Neurosci.* **19**, 3298 (1999).
8. G. Tamás, E. H. Buhl, A. Lörincz, P. Somogyi, *Nat. Neurosci.* **3**, 366 (2000).
9. C. E. Landisman *et al.*, *J. Neurosci.* **22**, 1002 (2002).
10. A. Simon, S. Oláh, G. Molnár, J. Szabadics, G. Tamás, *J. Neurosci.* **25**, 6278 (2005).
11. V. Zsiros, G. Maccaferri, *J. Neurosci.* **25**, 8686 (2005).
12. G. P. Dugué *et al.*, *Neuron* **61**, 126 (2009).
13. D. Schmitz *et al.*, *Neuron* **31**, 831 (2001).
14. F. Hamzei-Sichani *et al.*, *Proc. Natl. Acad. Sci. U.S.A.* **104**, 12548 (2007).
15. S. F. Stasheff, M. Hines, W. A. Wilson, *J. Neurophysiol.* **70**, 961 (1993).
16. R. D. Traub, S. B. Colling, J. G. R. Jefferys, *J. Physiol.* **489**, 127 (1995).
17. M. Avoli, M. Methot, H. Kawasaki, *Eur. J. Neurosci.* **10**, 2714 (1998).
18. J. O'Keefe, J. Dostrovsky, *Brain Res.* **34**, 171 (1971).
19. R. Muller, *Neuron* **17**, 813 (1996).
20. A. K. Lee, I. D. Manns, B. Sakmann, M. Brecht, *Neuron* **51**, 399 (2006).
21. A. K. Lee, J. Epsztein, M. Brecht, *Nat. Protoc.* **4**, 385 (2009).
22. J. Epsztein, A. K. Lee, M. Brecht, *Soc. Neurosci. Abstr.* **2008**, 690.21 (2008).
23. A. K. Lee, J. Epsztein, M. Brecht, *Soc. Neurosci. Abstr.* **2008**, 690.22 (2008).
24. S. Crochet, P. Fuentealba, I. Timofeev, M. Steriade, *Cereb. Cortex* **14**, 1110 (2004).
25. Materials and methods are available as supporting material on *Science* Online.
26. L. T. Thompson, P. J. Best, *J. Neurosci.* **9**, 2382 (1989).
27. C. D. Harvey, F. Collman, D. A. Dombeck, D. W. Tank, *Nature* **461**, 941 (2009).
28. A. Draguhn, R. D. Traub, D. Schmitz, J. G. Jefferys, *Nature* **394**, 189 (1998).
29. J. G. Jefferys, H. L. Haas, *Nature* **300**, 448 (1982).
30. C. P. Taylor, F. E. Dudek, *Science* **218**, 810 (1982).
31. J. L. Perez-Velazquez, T. A. Valiante, P. L. Carlen, *J. Neurosci.* **14**, 4308 (1994).
32. T. A. Valiante, J. L. Perez Velazquez, S. S. Jahromi, P. L. Carlen, *J. Neurosci.* **15**, 6946 (1995).
33. R. D. Traub, R. Bibbig, A. Piechotta, R. Draguhn, D. Schmitz, *J. Neurophysiol.* **85**, 1246 (2001).

34. We would like to thank B. Geue, R. Karpinski, and A. Stern at Humboldt University for technical assistance and D. Schmitz for comments on the manuscript. This work was supported by Neurocure, Bernstein Center for Computational Neuroscience (BMBF), Humboldt University, and Neuro-behavior European Research Council grants (M.B.), a European Molecular Biology Organization Long Term Fellowship (A.K.L.), and a Human Frontier Science Program Long Term Fellowship (J.E.).

Supporting Online Material

www.sciencemag.org/cgi/content/full/327/5964/474/DC1
Materials and Methods
Figs. S1 to S7

2 October 2009; accepted 3 December 2009
10.1126/science.1182773